Title
TEM STUDIES OF PRECIPITATE GROWTH AT THE ATOMIC LEVEL

Authors
Howe, J.M.
Gronsky, R.

Publication Date
1986

Lawrence Berkeley Laboratory
UNIVERSITY OF CALIFORNIA

Materials & Molecular Research Division

Presented at the Materials Research Fall Meeting, Boston, MA, December 2-7, 1985; and to be published in the Proceedings

TEM STUDIES OF PRECIPITATE GROWTH AT THE ATOMIC LEVEL

J.M. Howe and R. Gronsky

January 1986

Prepared for the U.S. Department of Energy under Contract DE-AC03-76SF00098

DISCLAIMER

TEM STUDIES OF PRECIPITATE GROWTH AT THE ATOMIC LEVEL

J.M. Howe and R. Gronsky*

Department of Metallurgical Engineering and Materials Science, Carnegie-Mellon University, Pittsburgh, PA 15213
*National Center for Electron Microscopy, Lawrence Berkeley Laboratory, University of California, Berkeley, California 94720

TEM STUDIES OF PRECIPITATE GROWTH AT THE ATOMIC LEVEL

J.M. HOWE and R. GRONSKY*

Department of Metallurgical Engineering and Materials Science, Carnegie-Mellon University, Pittsburgh, PA 15213
*National Center for Electron Microscopy, Lawrence Berkeley Laboratory, Berkeley, CA 94720

ABSTRACT

Recent advances in transmission electron microscopy instrumentation and technique now make it possible to study the shape-evolution of precipitates in metallic alloys at the atomic level. This investigation demostrates how a combination of transmission electron microscopy techniques; namely, high-resolution electron microscopy, image simulation, energy-dispersive x-ray spectroscopy and convergent-beam electron diffraction are used to characterize the atomic structures, chemistry and growth mechanisms of γ' precipitate plates in an Al-4.2 a/o Ag alloy aged for 30 min. at 350°C. The complimentary information obtained from each of these techniques allows modelling of the growth process at the atomic level, thus providing insight into the basic precipitation behavior of alloys.

1. INTRODUCTION

The interfacial structures and growth kinetics of γ' precipitate plates in Al-Ag alloys have been extensively studied by conventional and "in-situ" transmission electron microscopy (TEM) techniques, because the α(fcc) $\rightarrow$ γ'(hcp) transformation is one of the simpler diffusional transformations involving a distinct change in crystal structure[1-4]. Although these studies have provided considerable insight into the interfacial structures and growth behavior of plate-shaped precipitates, recent improvements in the high-resolution and probe-forming capabilities of TEM now provide the opportunity to study precipitation processes in metals at much greater levels of resolution than were previously possible[5,6]. In fact, this study demonstrates that the complimentary information obtained from high-resolution electron microscopy (HREM) and image simulations, energy-dispersive x-ray spectroscopy (EDS) and convergent-beam electron diffraction (CBED) allows the interfacial structure and growth mechanisms of γ' precipitates in an Al-Ag alloy to be understood at the atomic level. Because the mechanisms of precipitation in the Al-Ag system are analogous to those of many important commercial Al alloys and other alloy systems, understanding this model system provides insight into fundamental mechanisms controlling the growth behavior of precipitates in alloys.

2. EXPERIMENTAL PROCEDURES

An Al-4.2 a/o Ag alloy was solution annealed at 550°C, quenched in cold water, aged for 30 min. at 350°C and again quenched in cold water. Thin foils were polished in a nitric/methanol electrolyte and lightly ion-beam milled prior to insertion into a JEOL 200CX microscope for HREM. High-resolution images were taken both parallel and perpendicular to the faces of the γ' precipitates in $\langle 110\rangle//\langle 11\bar{2}0\rangle$ and $\langle 111\rangle//\langle 0001\rangle$ orientations, respectively. Simulated images of the precipitates and precipitate/matrix interface were calculated using the A.S.U. multislice programs[7]. The γ' precipitates were extracted from the Al matrix and their composition was analyzed on a Philips EM400 equipped with a Kevex System 7000 analytical spectrometer, using the ratio method[8] and an Ag_2Al standard. The CBED analyses were performed on a Philips EM400, which also had a "free lens" control[9,10] so that a wide range of convergence angles and probe diameters could be obtained on the specimens.

3. RESULTS AND DISCUSSION

3.1. Atomic Structure of Precipitate Faces in a $\langle 110\rangle//\langle 11\bar{2}0\rangle$ Orientation

Figures 1(a) and (b) show the projected potentials for two different types of dislocation ledges which are likely to be found on the faces of a γ' precipitate plate when it is viewed edge-on. These are called 30 and 90° Shockley partial dislocation ledges, based on the angles that their Burgers vectors make with the electron beam[11]. The γ' precipitate plates thicken by the movement of these dislocation ledges along their faces on alternate {111} matrix planes, which accomplishes the fcc → hcp structural transformation necessary for growth. Several simulated HREM images of these ledges are shown in Figs. 1(c) through (f). In Figs. 1(e) and (f), it is difficult to resolve the atomic positions at the edges of the ledges because alternate basal planes in the precipitate appear dark at this particular thickness and defocus condition. However, at a slightly different thickness, the atomic positions in both the precipitate and matrix are clearly visible, as demonstrated by Figs. 1(c) and (d).

Figure 2 shows an experimental HREM image of a multiple-unit ledge on the face of a γ' precipitate plate. Previous studies[4,5] have shown that elastic and diffusional interactions often cause single Shockley partial dislocation ledges on the precipitate faces to merge and form such multiple-unit ledges. Although it is difficult to distinguish the atomic positions at the edge of the ledge due to the particular thickness and defocus conditions in this image (compare with Figs. 1(e) and (f)), construction of an appropriate Burgers circuit indicates that four 30° Shockley partial dislocations are associated with this ledge. In addition, examination of the {111} matrix planes parallel to the precipitate face shows that they are continuous as they cross the edge of the multiple-unit ledge to become the {0001} precipitate planes and thus, that the edges of the ledges are largely coherent in this orientation, exactly as depicted in the models in Figs. 1(a) and (b). Also, slight displacement of these planes normal to the Burgers vectors of the ledge dislocations (perpendicular to the precipitate face) is evident, just as in the atomic models in Figs. 1(a) and (b). This type of displacement leads to the $\mathbf{g} \cdot \mathbf{b} \times \mathbf{u}$ contrast which is typically seen in strain contrast images of such dislocations[12].

Thus, from the matching between the calculated and experimental images of Shockley partial dislocation ledges in Figs. 1 and 2, it is possible to conclude that the structural transformation needed for growth of the γ' precipitates is accomplished by the passage of Shockley partial dislocations along alternate {111} matrix planes parallel to the faces, and that the growth interface is essentially coherent in this orientation.

3.2. Atomic Structure of Precipitate Edges in a <110>//<11$\bar{2}$0> Orientation

Figure 3 shows a HREM image of a precipitate edge in a <110>//<11$\bar{2}$0> orientation. The stepped-down shape of this edge indicates that it is composed of Shockley partial dislocations which have migrated across the precipitate faces and assumed a staggered configuration at the edge. Again, sighting along the {111} planes parallel to the faces shows that the edge is largely coherent, just as for the ledges on the faces described above, although some of the atom planes bend significantly as they cross the interface into the precipitate. These image characteristics agree with a precipitate edge that is modelled as being composed of Shockley partial dislocations which are stacked vertically, although it is difficult to distinguish the positions of the individual partial dislocations at the edge due to the complex nature of this interface and the fact that some matrix is overlapping the precipitate edge and confusing the atomic detail. Also notice that the precipitate edge in Fig. 3 is nearly flat, rather than having a semicircular or parabolic-cylinder shape, as is often assumed in kinetic analyses of precipitate plate lengthening[13].

Several crystallographic planes in the matrix are also indicated in the top-left corner in Fig. 3, and comparing these planes with the precipitate edge shows that the edge parallels a {112} matrix plane overall. However, close examination reveals that this nearly planar interface is further faceted along {111} matrix planes, and that these {111} facets have a six-plane repeating pattern, which is also indicated in Fig. 3. This six-plane repeating pattern is particularly interesting because it appears to directly relate to the way in which the fcc → hcp structural transformation for precipitate growth occurs. As illustrated by Fig. 4, a hcp precipitate could thicken either by the nucleation and propagation of the same Shockley partial dislocations on alternate {111} matrix planes (Fig. 4(a)), or by the generation of equal numbers of all three possible variants of Shockley partial dislocations on alternate {111} planes (Fig. 4(b)). However, the latter situation is highly favored from strain energy considerations, since the strain fields associated with the three variants of Shockley partial dislocations will cancel when the dislocations merge at the edges and thus, eliminate long-range strains parallel to the habit plane of the precipitate. Notice that the six-plane pattern which is formed when all three variants of Shockley partial dislocations participate in the growth process in Fig. 4(b) is identical to the six-plane repeating pattern at the precipitate edge in Fig. 3, demonstrating that the influence of the elastic strain energy is sufficient to ensure that all three variants of Shockley partial dislocations are nucleated in roughly equal numbers, in order to minimize the elastic strain energy at the precipitate edges.

3.3. Atomic Structure of Edges in a <111>//<0001> Orientation

The edges of the γ' precipitates were also examined using HREM, with the precipitates oriented face-on with respect to the electron beam. These studies were performed in order to characterize the atomic structure and coherency of the precipitate edges in a direction perpendicular to the previous analyses, or along the third dimension of the precipitates. Although it is possible to resolve the atomic positions within the precipitates using axial illumination in this orientation, it was necessary to tilt the incident electron beam so that the first-order 1.4 Å {220} matrix planes could be resolved in order to determine the coherency of the precipitate edges[14]. Fig. 5 shows a corner at the edge of a γ' precipitate, taken in the tilted-illumination condition. Sighting along the {220} matrix planes reveals that they are continuous as they cross the interface to become the $\{11\bar{2}0\}$ precipitate planes, which demonstrates that the precipitates are coherent with the matrix in the habit plane.

Figure 6 shows a second tilted-illumination, high-resolution image of several single-plane ledges spaced about 35 Å apart along the edge of a γ' plate. Two particular features are important in this image. First, the edges of the precipitate plate are faceted along low-energy <110> directions within the {111} matrix plane (and corresponding low-energy $\langle 11\bar{2}0\rangle$ directions within the {0001} precipitate plane) at the atomic level. This behavior indicates that interfacial energy effects strongly influence the morphology of the precipitates[15,16]. This influence is further reflected by the fact that the γ' precipitates usually assume a hexagonal shape within the habit plane[3,4]. Secondly, the terraces between each of the ledges in Fig. 6 are atomically flat while the edges of the ledges (arrows) are indistinct, indicating that atomic attachment is occurring at the edges of the ledges. However, because each of these ledges actually represents a kink in a Shockley partial dislocation when all three dimensions are considered, this image further suggests that growth of the γ' precipitates occurs by the attachment of atoms to kinks in the Shockley partial dislocations, which constitute the ledges on both the faces and edges of these precipitate plates. Thus, the classic terrace-ledge-kink mechanism of atomic attachment which was originally proposed for the growth of close-packed interfaces of a solid into a liquid or vapor[17], appears to be equally valid for describing the growth of a close-packed solid of one crystal structure into another[18].

3.4. Quantitative EDS Analyses of Extracted Precipitates

Figure 7 compares a typical EDS spectrum from an extracted γ' precipitate with a similar spectrum obtained from an Ag_2Al (66 a/o Ag) standard. Although the Ag_2Al spectrum contains nearly twice a many counts as the precipitate spectrum, inspection of the ratios of the heights of the Al Kα to the Ag Kα peaks shows that they are about 2.5:1 for both specimens. A value for $k_{\alpha AgAl}$ was determined by analyzing several spectra from the Ag_2Al standard. The composition of the γ' precipitates was then determined to be 66.8 ± 3.8 a/o Ag by analyzing the spectra from ten precipitates using the ratio method. Thus, the composition of these metastable γ' precipitates is similar to the congruently melting compound Ag_2Al present in the Al-Ag equilibrium phase diagram[19]. This composition lies near the Ag-rich side of the equilibrium γ phase field at 350°C, and is the composition usually assigned to equilibrium γ precipitates which form in Al-Ag alloys after extended high-temperature aging treatments[20].

3.5. CBED of Precipitates in a <110>//<11$\bar{2}$0> Orientation

Although it has not been mentioned until now, a light-to-dark contrast change occurs between every other basal plane in the previous <110>//<11$\bar{2}$0> HREM images, indicating that the γ' precipitates may possess long-range order among alternate basal planes. Such order should lead to the appearance of kinematically forbidden 000l, l=odd precipitate reflections in diffraction patterns from precipitates, and these reflections were often found in the selected area diffraction patterns recorded with the HREM images. However, the 000l, l=odd reflections can also appear due to double diffraction in the precipitate and therefore, caution must be exercised when deciding on the origin of these reflections[21]. In this study CBED was used to determine whether the 000l, l=odd reflections were due to ordering or double diffraction. Fig. 8 shows two <110>//<11$\bar{2}$0> CBED patterns taken from different precipitates located a short distance from one another in the foil. In Fig. 8(a), the 000l, l=odd reflections are strong and there is no evidence of Gjonnes-Moodie (G-M) lines[22], indicating that the reflections are not kinematically or dynamically forbidden and therefore, that they are due to long-range order on alternate basal planes in the precipitate. However, the same 000l, l=odd reflections in Fig. 8(b) display clear G-M lines through their centers due to the presence of a c-glide plane, indicating that these reflections are kinematically forbidden and therefore, that this precipitate does not possess long-range order among alternate basal planes. These apparently conflicting results can be explained by assuming that individual γ' precipitates possess various degrees of order, ranging from a highly-ordered arrangement of Ag and Al atoms on alternate basal planes to a disordered arrangement. This behavior is also consistent with the observation that γ' precipitates undergo a order/disorder transformation at the 350°C aging temperature[1].

3.6. Simulated Images of Precipitates and Precipitate/Matrix Interface

The previous sections demonstrated how HREM, EDS and CBED could be used to to obtain detailed information about the interfacial structure, chemical composition and degree of order of the γ' precipitates. In this section, the information obtained from each of these techniques is combined, in order to construct an atomic model of the γ' precipitates and the precipitate/matrix interface. The validity of this model is then determined by comparing simulated HREM images of these features with corresponding experimental images. Only a few of the many images[14,21], which were calculated in order to investigate the effects of: 1) composition between alternate basal planes, 2) specimen thickness, 3) objective lens defocus, 4) specimen tilt, and 5) beam tilt on the amplitudes and phases of the diffracted beams and resulting image contrast, are presented herein.

Figure 9 shows one series of calculated images for a precipitate/matrix interface in a <110>//<11$\bar{2}$0> orientation. The model for this interface is shown by the projected potential in the top-left corner of Fig. 9. In this model, the A-planes in the precipitate are nearly pure Ag while the B-planes contain 33 a/o Ag with a balance of Al. Thus, the precipitate has an average composition of 66 a/o Ag as given by the EDS analyses, but also possesses long-range order among alternate basal planes, as indicated for some precipitates by the CBED analyses and HREM images. The precipitate/matrix interface is between the last Ag-rich, A-plane in the precipitate and the first B-plane in the matrix. By examining the images in Fig. 9, it

is apparent that for certain values of objective lens defocus and specimen thickness, such as at -1460 Å defocus and 37.2 Å thickness, it is possible to determine the atomic structure of both the precipitate and precipitate/matrix interface. For example, examination of the structure of the precipitate in this image shows that moving from an atom position in the dark A-plane to a bright atom position in the B-plane above, requires a translation of 1/3 of the lattice spacing to the right. Additional examination of the matrix in this image shows that the stacking sequence of the A,B and C-planes occurs by the translation of atoms 1/3 of the lattice spacing to the right, verifying that the A and B-planes in the precipitate were correctly chosen and therefore, that the A planes are Ag-rich.

Figure 10 shows an experimental HREM image of a γ' precipitate/matrix interface in a $\langle 110\rangle//\langle 11\bar{2}0\rangle$ orientation. The amorphous layer at the edge of the foil is just visible in the left side of this figure, and the corresponding electron and optical diffraction patterns are also shown. Comparing the spatial frequencies of the specimen and halos in the optical diffraction pattern in Fig. 10 with the contrast transfer function[23] (CTF) in Fig. 11, indicates that this image was taken at about -1440 Å defocus. At this objective lens defocus, all of the first-order precipitate and matrix reflections are imaged by the objective lens with roughly the same phase and amplitude ($\sin\chi = 1$) and thus, this defocus condition represents an optimum setting for the spatial frequencies of the specimen. In addition, examination of the HREM image shows that the brightness of the atoms in the darker plane of the precipitate slowly decreases from left to right in the micrograph. Comparison of this contrast change with the simulated images in Fig. 9 shows that good agreement is obtained for a sample thickness which varies from about 20 Å at the edge to about 40 Å on the right side of the micrograph. This is clearly illustrated by the inset smulated image of the interface at -1440 Å defocus and 37.2 Å thickness shown in Fig. 10. Thus, the matching between the experimental and simulated images indicates that the model for the precipitate and interface shown by the projected potential in Fig. 9 is correct.

3.7. Atomic Mechanisms of Precipitate Plate Growth

Now that the structure and chemistry of γ' precipitates and the precipitate/matrix interface have been determined at the atomic level, it is possible to further establish the relationship between the structural and chemical components of the transformation, thus enabling growth of the γ' precipitates to be described at the atomic level. Fig. 12 shows an enlargement of the projected potential previously discussed in Fig. 9. The γ' precipitate in this model is composed of A-planes that are pure Ag and B-planes that contain 33 a/o Ag. The stacking sequences in both the precipitate and matrix are also labelled, and the precipitate/matrix interface is indicated by a solid line. In order for the precipitate to thicken, two processes must occur: 1) a Shockley partial dislocation must propagate along the C-plane in the matrix and translate these atoms into A-positions, and 2) there must be a corresponding chemical change which allows the A-planes in the precipitate to contain pure Ag and the B-planes to contain 33 a/o Ag. Thus, both the structural and major chemical changes which are necessary for growth of the precipitate occur in the same atom plane. In addition, since it was previously shown that both the thickening and lengthening of γ' precipitate plates appears to occur by the movement of kinks in Shockley partial dislocation ledges, it is possible to further infer that the growth of γ' precipitates occurs by the substitutional diffusion of Ag

atoms across kinks in the Shockley partial dislocation ledges, and that this is the limiting reaction in the growth process.

It is also apparent from Fig. 12, that the B-plane in the two-plane ledge does not undergo a structural transformation as the Shockley partial dislocation propagates along the interface. Consequently, substitutional diffusion of Ag within this plane at the edge of the ledge is roughly independent of ledge structure, indicating that structural aspects of the transformation such as the disorder associated with the kinks and their density along the ledges mainly need to be considered for only the upper-atom plane in a two-plane ledge. In addition, because the B-plane possesses the required structural arrangement for the hcp precipitate before the Shockley partial dislocation passes along the interface, significant compositional changes may occur in this plane prior to its incorporation into the precipitate. Thus, while previous kinetic analyses have been highly successful in predicting the growth rates of both the edges and ledges on the faces of precipitate plates by assuming that they are disordered interfaces[24,25], the observations in this study indicate that many subtle but important aspects of the transformation need to be taken into account in order to understand and accurately model the growth process on an atomic level.

4. CONCLUSIONS

The purpose of the present research was to perform highly detailed analyses of both the structural and chemical components required for growth of γ' plate-shaped precipitates in an Al-Ag alloy, in order to understand the mechanisms of precipitate growth at the atomic level. In order to accomplish this, the techniques of HREM and image simulations, EDS microanalysis and CBED were employed. The major findings of this study are: **1)** comparison between experimental and simulated HREM images of Shockley partial dislocation ledges shows that both the faces and edges of γ' precipitate plates grow by the passage of Shockley partial dislocations along alternate {111} matrix planes, **2)** the elastic strain energy associated with the fcc $\rightarrow$ hcp structural transformation is minimized by the nucleation of equal numbers of all three variants of Shockley partial dislocations on the same {111} faces of precipitates, **3)** all interfaces of γ' precipitates are largely coherent and faceted along low-energy $\langle 111\rangle // \langle 0001\rangle$ and $\langle 110\rangle // \langle 11\bar{2}0\rangle$ directions, thereby minimizing both the chemical and structural interfacial energies associated with the interphase boundary, **4)** the composition of the γ' precipitates is Ag_2Al, and the precipitates possess long-range order on alternate basal planes during the early stages of growth at 350°C, where the A-planes in the precipitates contain nearly pure Ag and the B-planes have the composition Al_2Ag, and **5)** agreement between experimental and calculated HREM images of the precipitate/matrix interface indicates that the limiting reaction in the growth process is the substitutional diffusion of Ag atoms across kinks in the Shockley partial dislocations ledges, which terminate in the Ag-rich, A-planes of the precipitate.

ACKNOWLEDGEMENTS

This research was supported by the Director, Office of Energy Research, Office of Basic Energy Sciences, Materials Science Division of the U.S. Department of Energy under Contract No. DE-AC03-76SF00098.

REFERENCES

1. J.A. Hren and G. Thomas, TMS-AIME, 227, 308 (1963).

2. R.B. Nicholson and J. Nutting, Acta Met., 9, 332 (1961).

3. C. Laird and H.I. Aaronson, Acta Met., 15, 73 (1967).

4. J.M. Howe, H.I. Aaronson and R. Gronsky, Acta Met., 33, 639 (1985).

5. J.M. Howe, H.I. Aaronson and R. Gronsky, Acta Met., 33, 649 (1985).

6. R. Gronsky, G. Van Tendeloo and G. Thomas, presented at the Acta/Scripta Conference, Sonnenberg, Germany, 1983 (LBL Report No. 17369, 1984).

7. M.A. O'Keefe and P.R. Buseck, Trans. Amer. Cryst. Assoc., 15, 27 (1979).

8. G. Cliff and G.W. Lorimer, J. Microscopy, 110, 107 (1975).

9. M. Sarikaya and G. Thomas, in *Analytical Electron Microscopy*, edited by D.B. Williams and D.C. Joy (San Francisco Press, San Francisco, 1984), p. 97.

10. J.M. Howe, M. Sarikaya and R. Gronsky, submitted to Acta Cryst.

11. J.P. Hirth and H. Lothe, *Theory of Dislocations*, 2nd ed. (John Wiley and Sons, New York, 1982), p. 315.

12. Sir P. Hirsch, A Howie, R.B. Nicholson, D.W. Pashley and M.J. Whelan, *Electron Microscopy of Thin Crystals*, 2nd ed. (Robert E. Krieger Pub., Malibar, 1977), p. 178.

13. H.I. Aaronson, J.K. Lee and K.C. Russell, in *Precipitation Processes in Solids*, edited by K.C. Russell and H.I. Aaronson, (TMS-AIME, Warrendale, 1977), p. 31.

14. J.M. Howe, Ph.D. Thesis, University of California, Berkeley, 1985.

15. F.K. LeGouges, R.N. Wright, Y.W. Lee and H.I. Aaronson, Acta Met., 32(10), 1865 (1984).

16. J.W. Christian, *The Theory of Transformations in Metals and Alloys*, 1st ed. (Pergamon Press, Oxford, 1965), p. 142.

17. W.K. Burton, N. Cabrera and F.C. Frank, Phil. Trans. Roy. Soc. London, A243, 299 (1950-51).

18. H.I. Aaronson, in *Decomposition of Austenite by Diffusional Processes*, edited by V.F. Zackay and H.I. Aaronson, (Interscience Pub., New York, 1962), p. 387.

19. Bulletin of Alloy Phase Diagrams, 1(1), 36 (1983).

20. L.F. Mondolfo, *Aluminum Alloys: Structure and Properties*, 1st ed. (Butterworths, London, 1979), p. 213.

21. J.M. Howe and R. Gronsky, to be published in Ultramicroscopy.

22. J. Gjonnes and A.F. Moodie, Acta Cryst., 19, 65 (1965).

23. R. Kilaas, unpublished research (1984).

24. C. Laird and H.I. Aaronson, Acta Met., 17, 505 (1969).

25. C. Laird and H.I. Aaronson, TMS-AIME, 242, 1437 (1968).

FIGURE CAPTIONS

Figure 1. (a) and (b) Projected potentials for single 90 and 30° Shockley partial dislocation ledges on the face of a γ' precipitate, respectively, (c) and (d) corresponding simulated HREM images for a foil thickness of 34.4 Å and an objective lens defocus of -1460 Å, and (e) and (f) simulated images for a foil thickness of 71.6 Å and an objective lens defocus of -1460 Å. The dislocation cores are circled and the stacking sequences on both sides of the ledges are indicated in the projected potentials.

Figure 2. Experimental $\langle 110\rangle//\langle 11\bar{2}0\rangle$ HREM image of an approximately ten-plane ledge on the face of a γ' precipitate, with a Burgers circuit that indicates the presence of four 30° Shockley partial dislocations associated with the ledge.

Figure 3. HREM image of a precipitate edge in a $\langle 110\rangle//\langle 11\bar{2}0\rangle$ orientation showing that: 1) the nearly planar edge parallels a {112} plane in the matrix, 2) the edge is further faceted along {111} matrix planes, and 3) the {111} facets have a six-plane repeating pattern. The origin of the six-plane pattern is discussed further with reference to Figure 4.

Figure 4. Illustration of two different ways of transforming cubic close-packed planes into hexagonal close-packed planes: (a) using the same Shockley partial dislocation on alternate (111) planes, and (b) using equal numbers of all three types of Shockley partial dislocations on alternate (111) planes. Each block represents two (111) matrix planes.

Figure 5. A $\langle 111\rangle//\langle 0001\rangle$ tilted-illumination, high-resolution image at the corner of a γ' precipitate. The 1.4 Å {220} matrix planes are continuous as they cross the interphase boundary to become the $\{11\bar{2}0\}$ precipitate planes, demonstrating that the precipitate/matrix interface is coherent in this orientation.

Figure 6. A second tilted-illumination image which shows a series of single-atom ledges migrating along the precipitate edge. The edges of the ledges (arrows) are diffuse while the terraces between the ledges are atomically flat.

Figure 7. (a) EDS spectrum from an extracted γ' precipitate, and (b) comparative spectrum from an Ag_2Al standard, (c) through (f) enlargements comparing the relative sizes of the Al Kα and Ag Kα peaks from the precipitate and standard, respectively. The large Cu peak in (a) is due to flourescence from the supporting Cu grid.

Figure 8. (a) and (b) Two $\langle 110\rangle//\langle 11\bar{2}0\rangle$ CBED patterns from γ' precipitates located a short distance apart in the same thin foil. The 000l, l=odd precipitate reflections in (a) display strong intensities indicating that they are allowed, while the same reflections in (b) contain G-M lines indicating that they are forbidden.

Figure 9. Simulated images of a γ' precipitate/matrix interface as a function of objective lens defocus and specimen thickness. The γ' precipitate contains pure Ag on the A-planes and 33 a/o Ag on the B-planes, and the images were calculated with: C_s = 1.2 mm, Δ = 50 Å, α_i = 1.0 mrad and Acc. Volt. = 200 keV.

Figure 10. Experimental HREM image of a γ' precipitate/matrix interface in a $\langle 110\rangle // \langle 11\bar{2}0\rangle$ orientation, with the corresponding electron and optical diffraction patterns. A matching simulated image of the interface at -1440 Å and 37.2 Å defocus is superimposed on the experimental image.

Figure 11. CTF for the JEOL 200CX microscope at -1440 Å defocus with the following microscope conditions: C_s = 1.2 mm, Δ = 50 Å, α_i = 0.5 mrad and Acc. Volt. = 200 keV. The spatial frequency of the 0001 precipitate reflection at 0.21 $Å^{-1}$, and the frequencies of the 0002, $01\bar{1}0$, $01\bar{1}1$ precipitate reflections and the 111 and 020 matrix reflections, which lie between 0.40 to 0.50 $Å^{-1}$, are indicated on the axis where the CTF = 0.

Figure 12. Illustration showing how the structural and major chemical changes needed for growth of a γ' precipitate plate occur in the same atomic plane when the A-planes of the precipitate are Ag-rich and the Shockley partial dislocation propagates along the C-plane in the matrix.

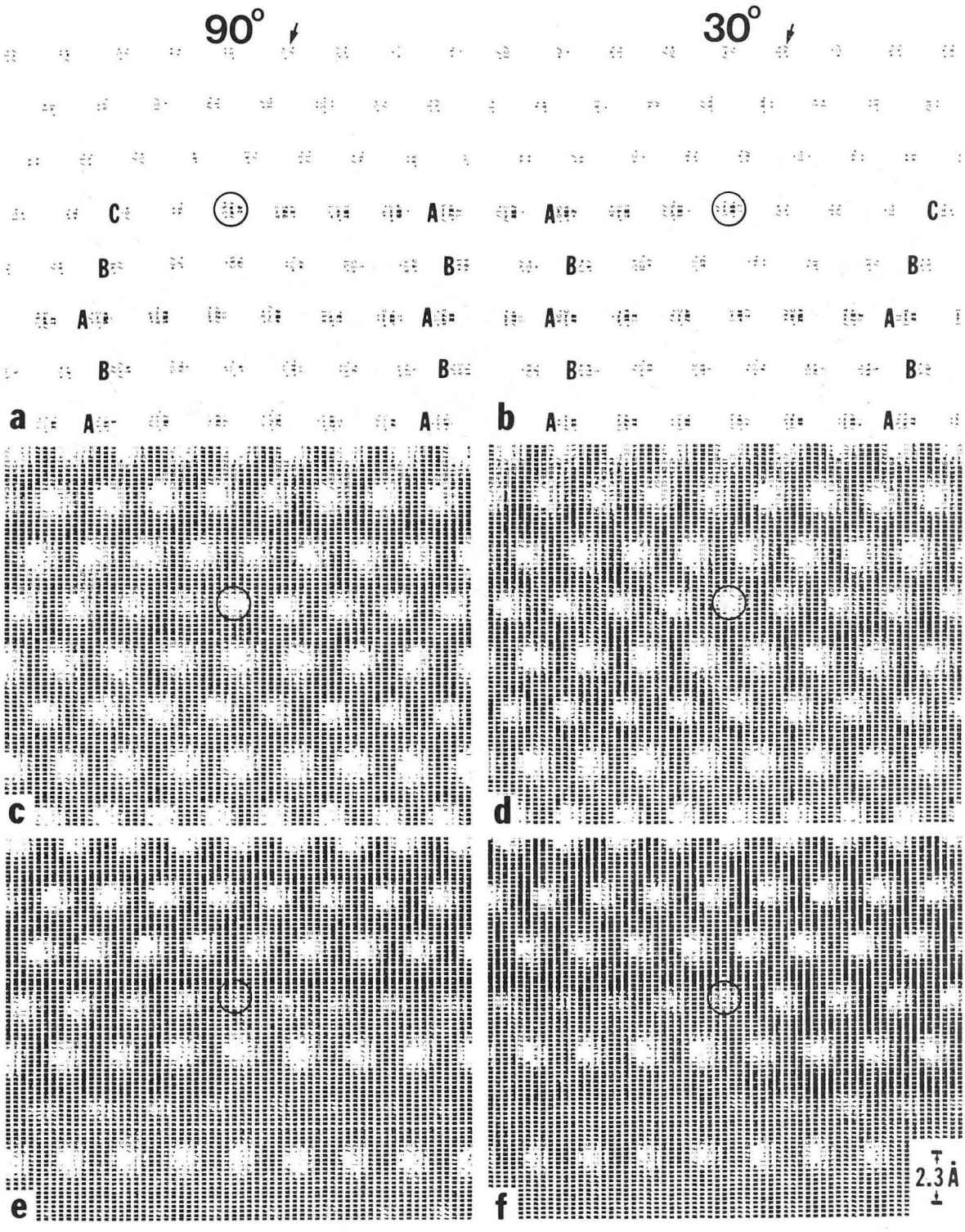

XBL 857-3141

Fig. 1

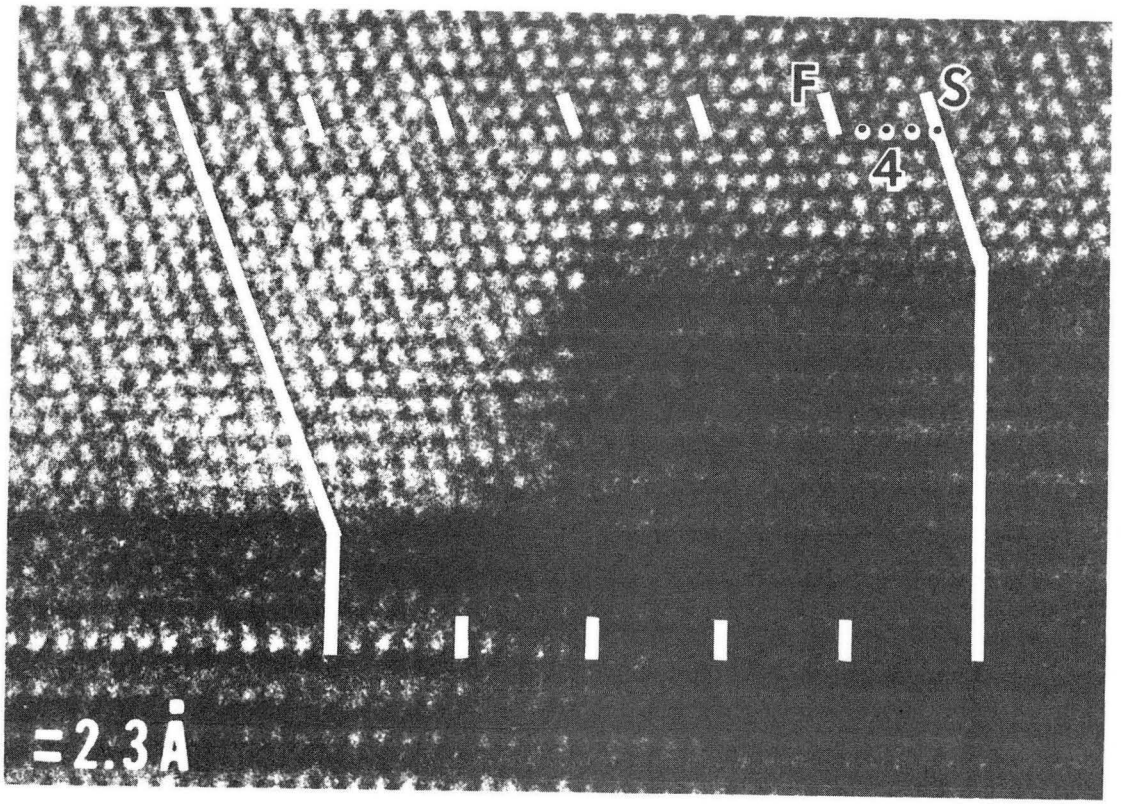

XBB 830-10305B

Fig. 2

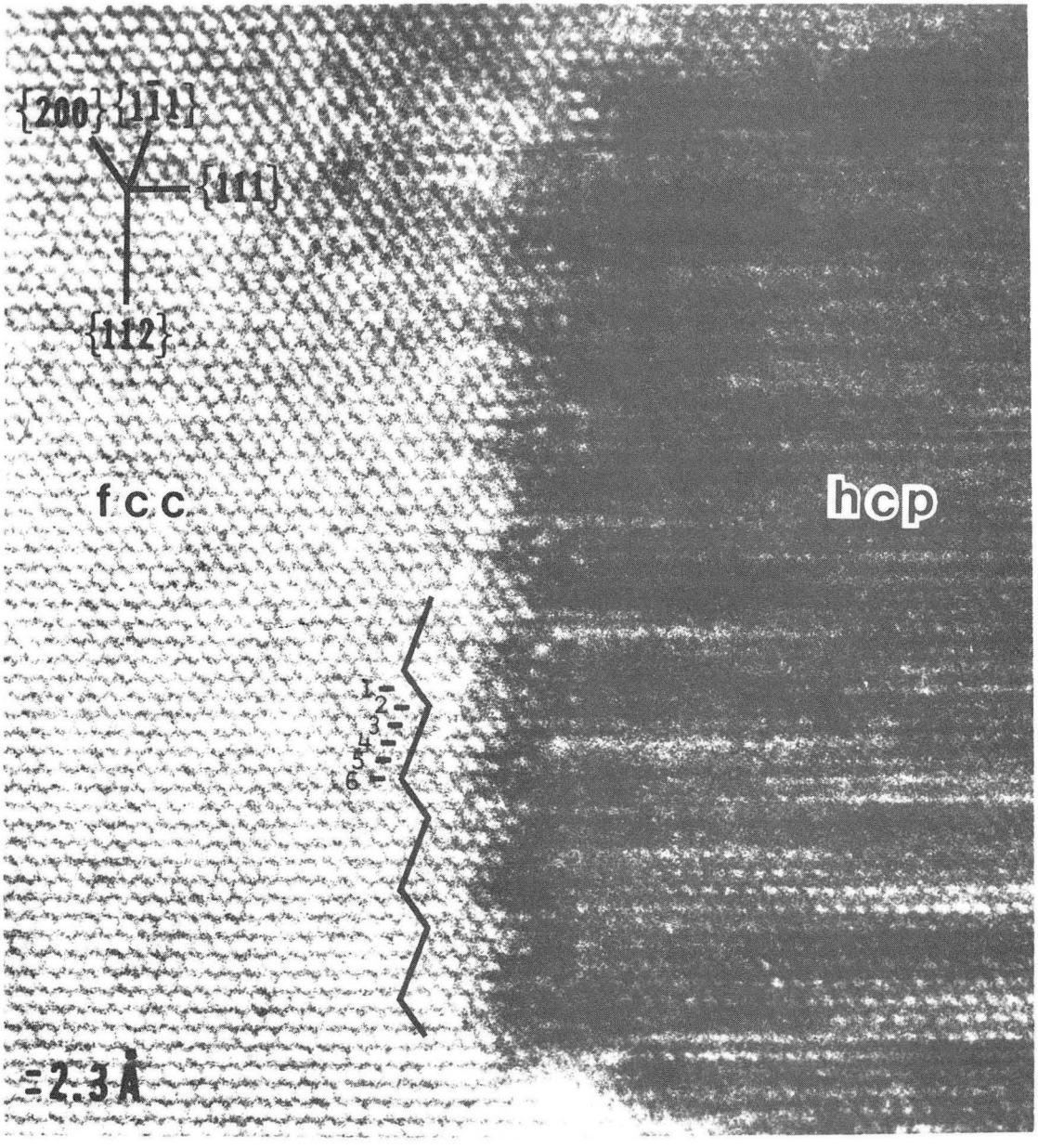

XBB 857-5316A

Fig. 3

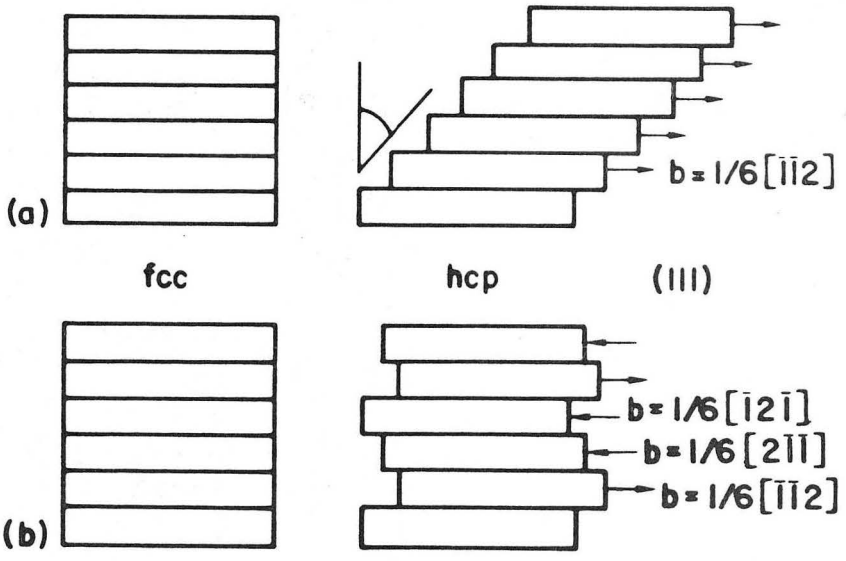

XBL 841-10016

Fig. 4

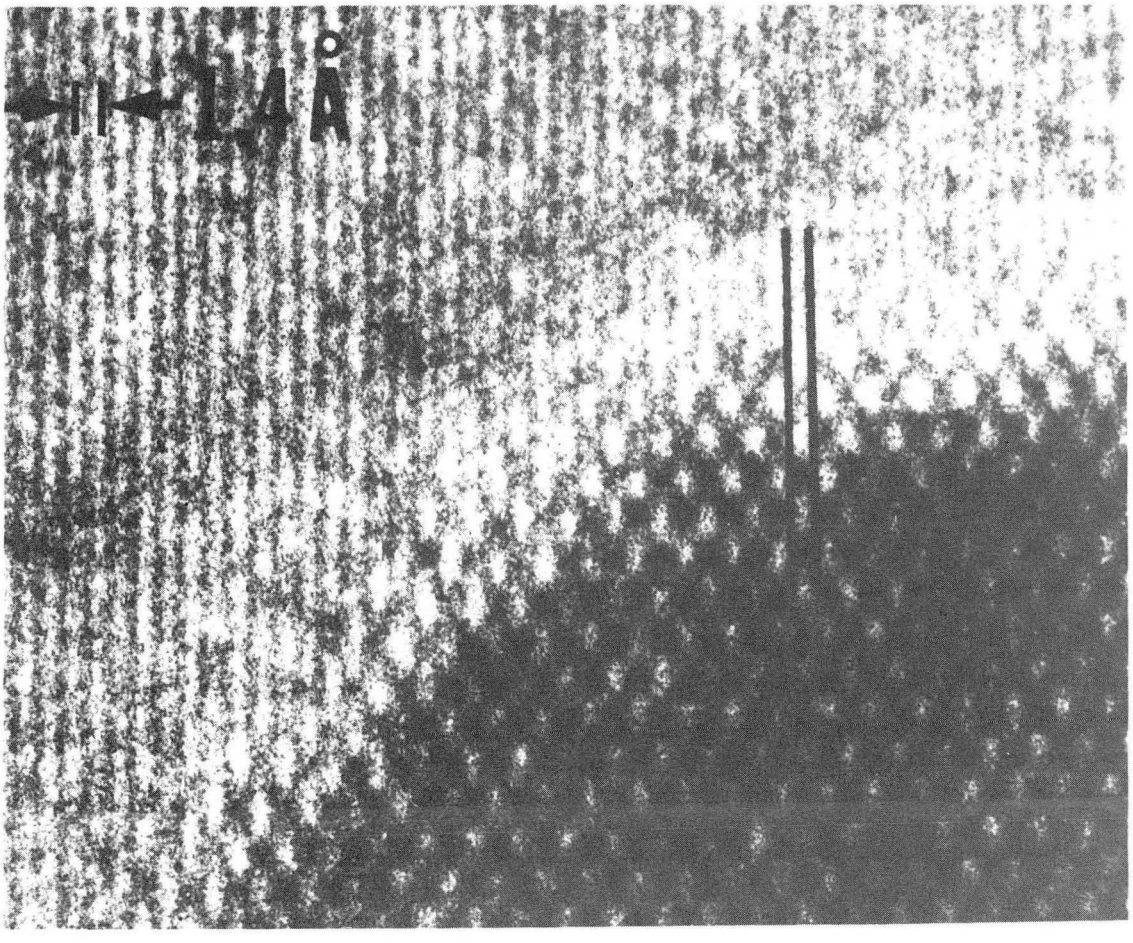

XBB 842-1204

Fig. 5

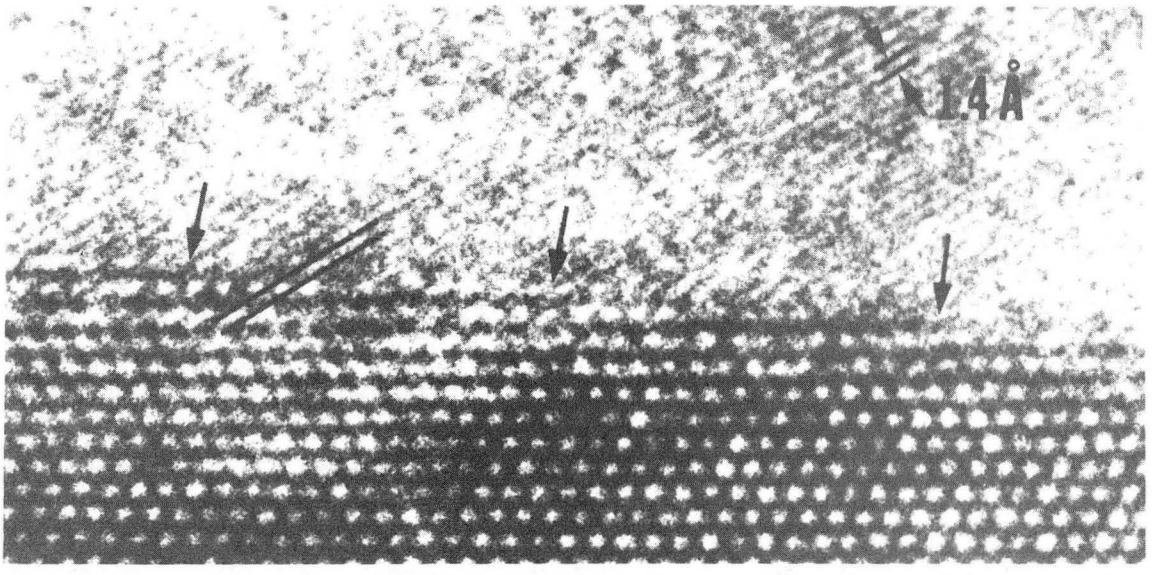

XBB 842-1205

Fig. 6

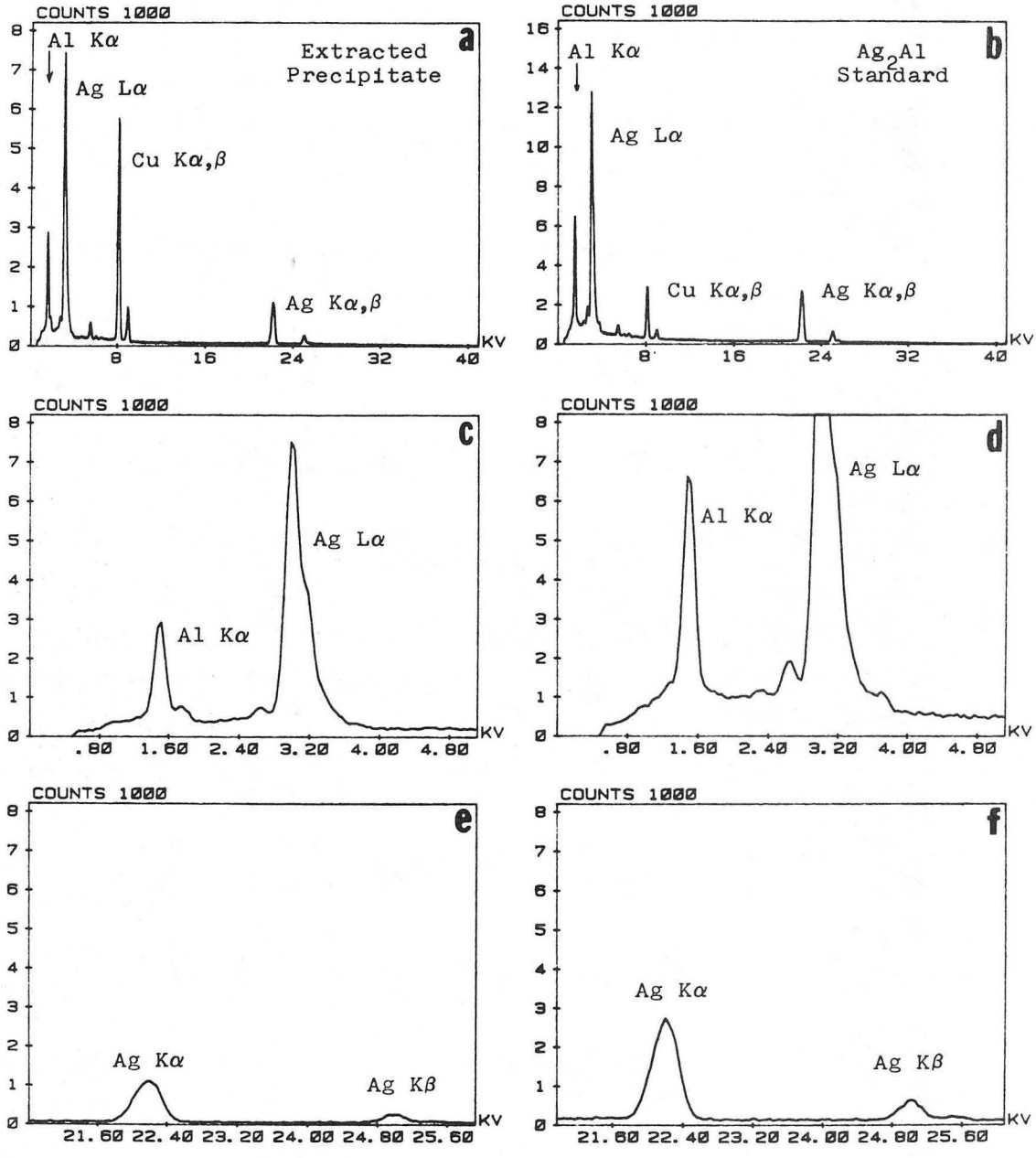

XBL 8410-4157

Fig. 7

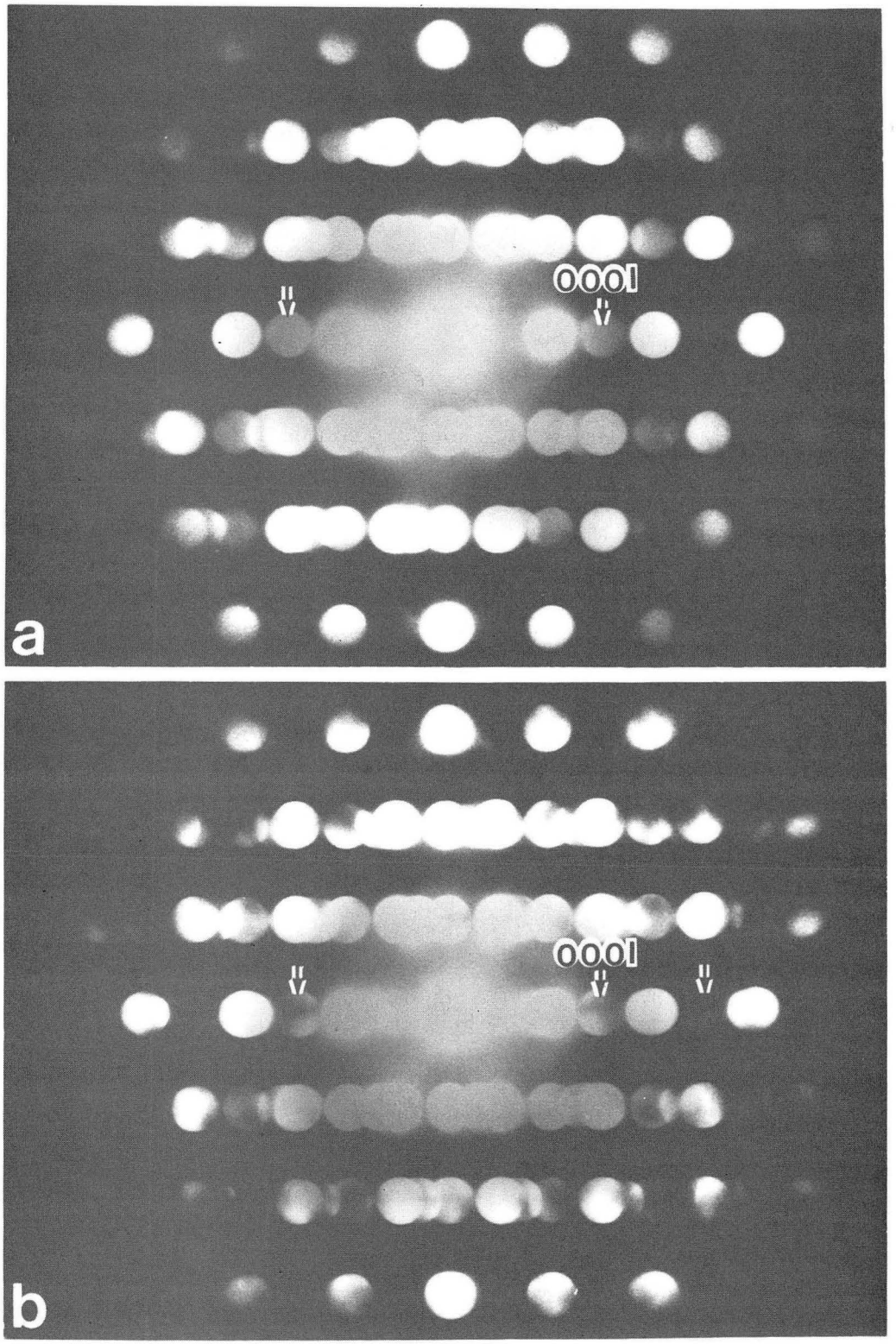

XBB 856-5646

Fig. 8

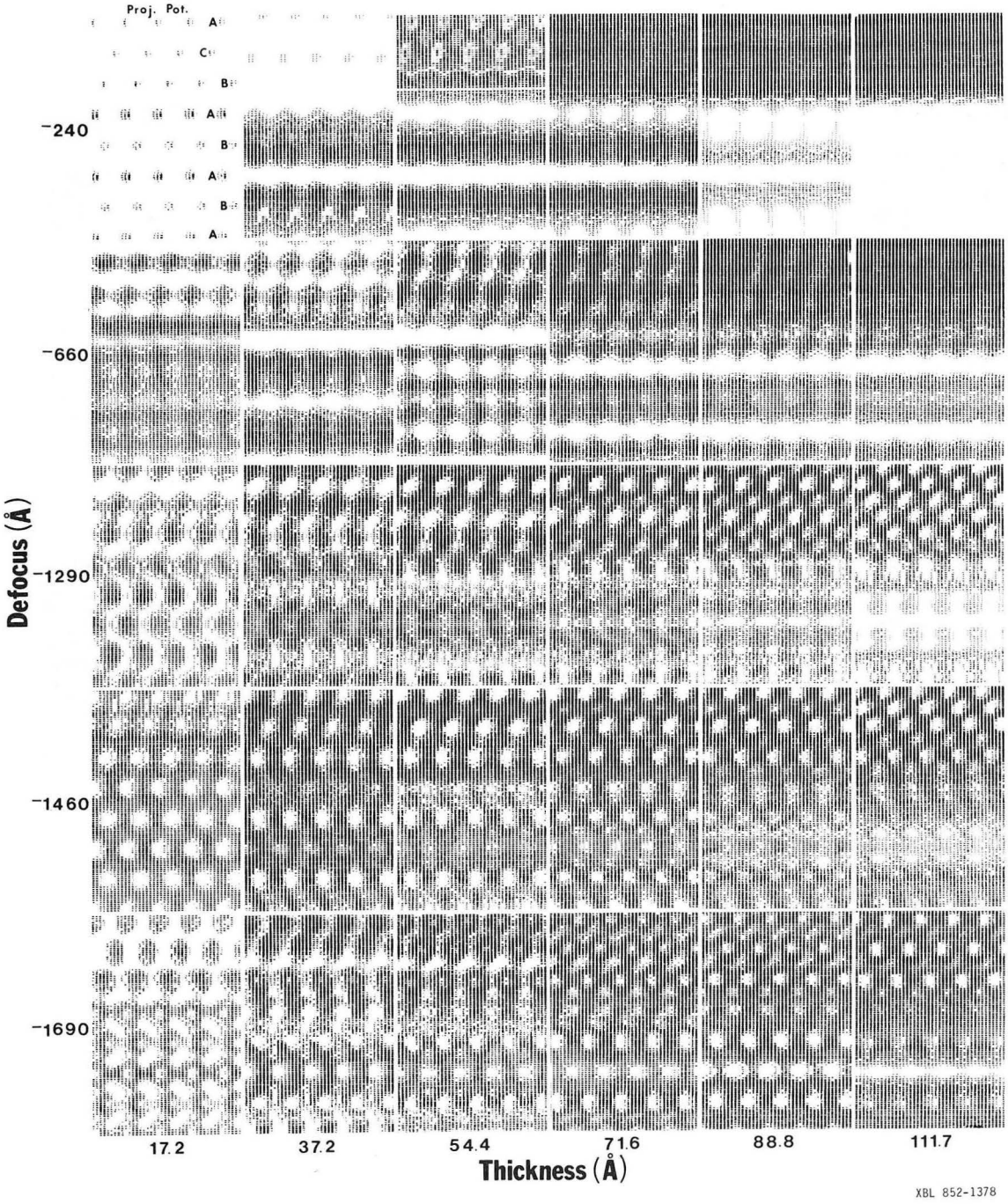
Proj. Pot.
A
C
B
A
B
A
B
A
-240
-660
-1290
-1460
-1690
Defocus (Å)
17.2
37.2
54.4
71.6
88.8
111.7
Thickness (Å)
XBL 852-1378

Fig. 9

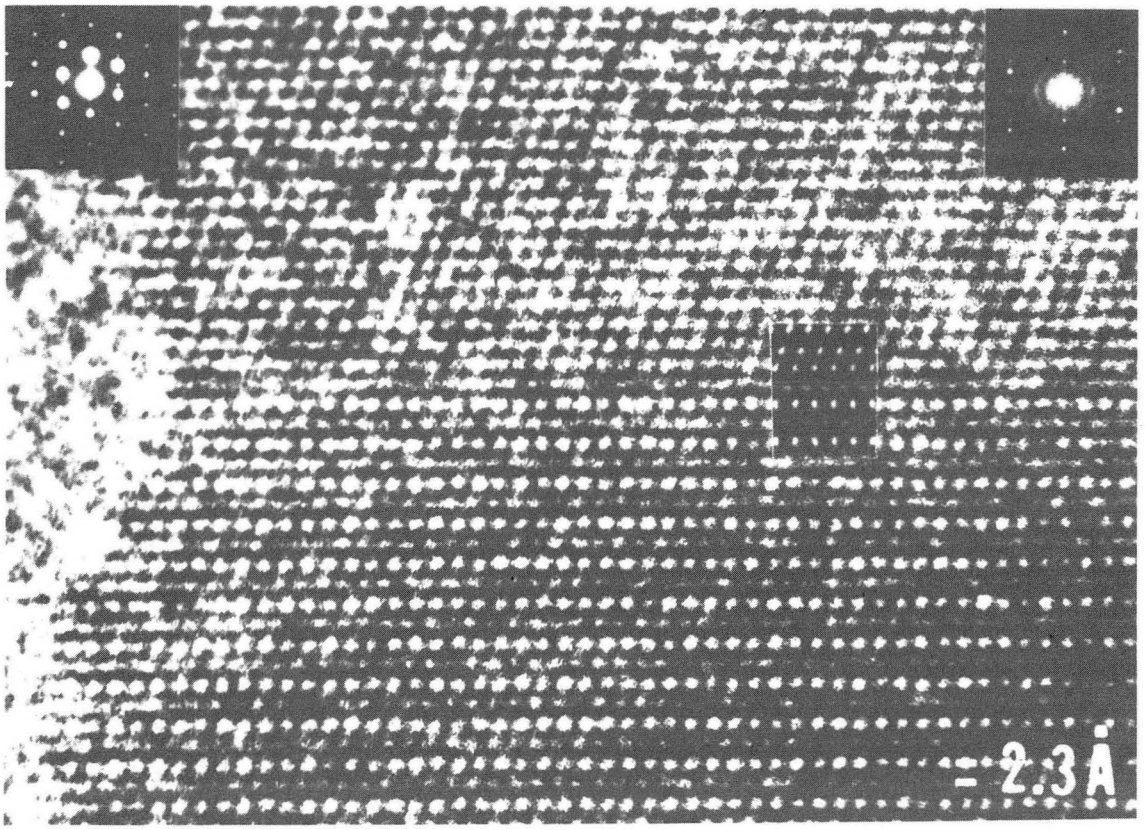

XBB 846-4293

Fig. 10

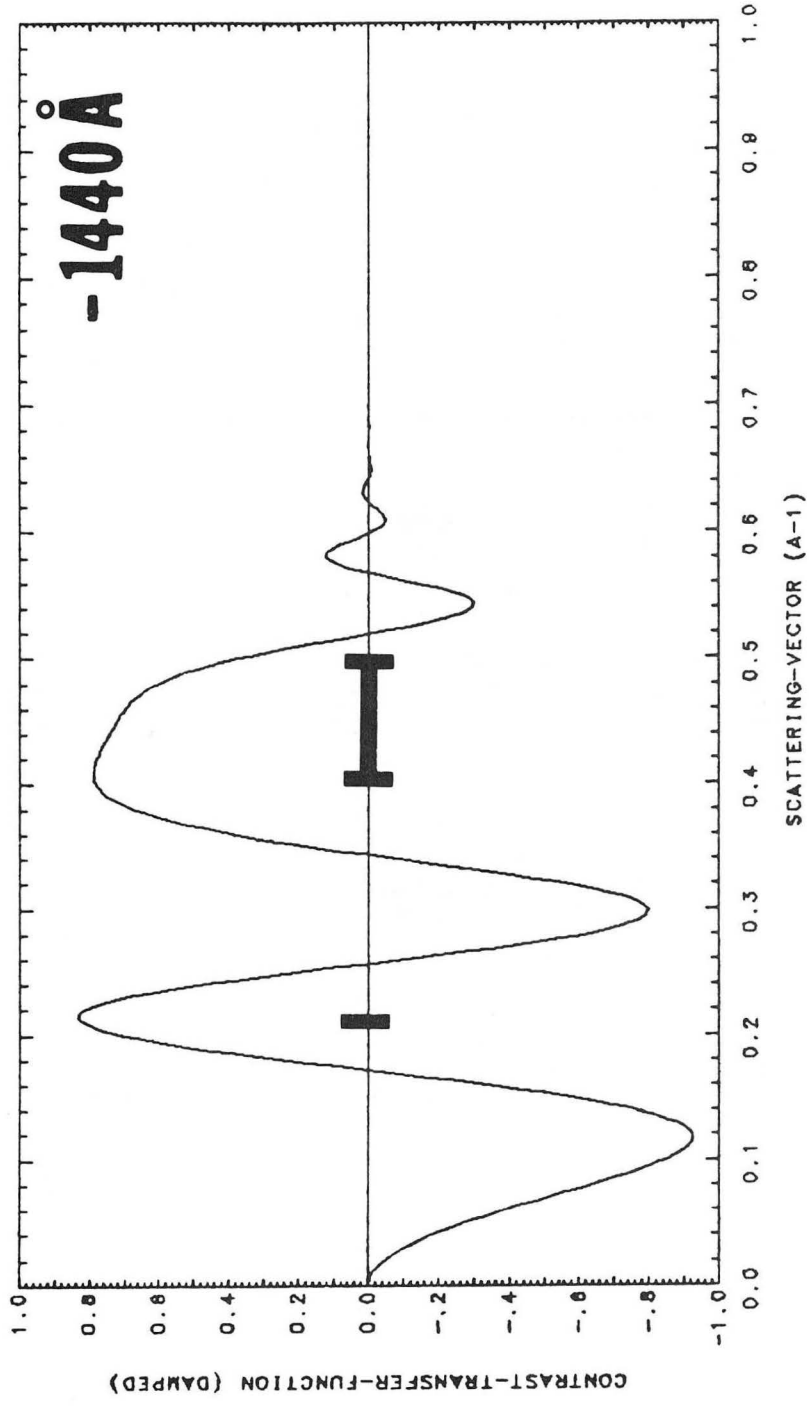

XBL 8511-4501

Fig. 11

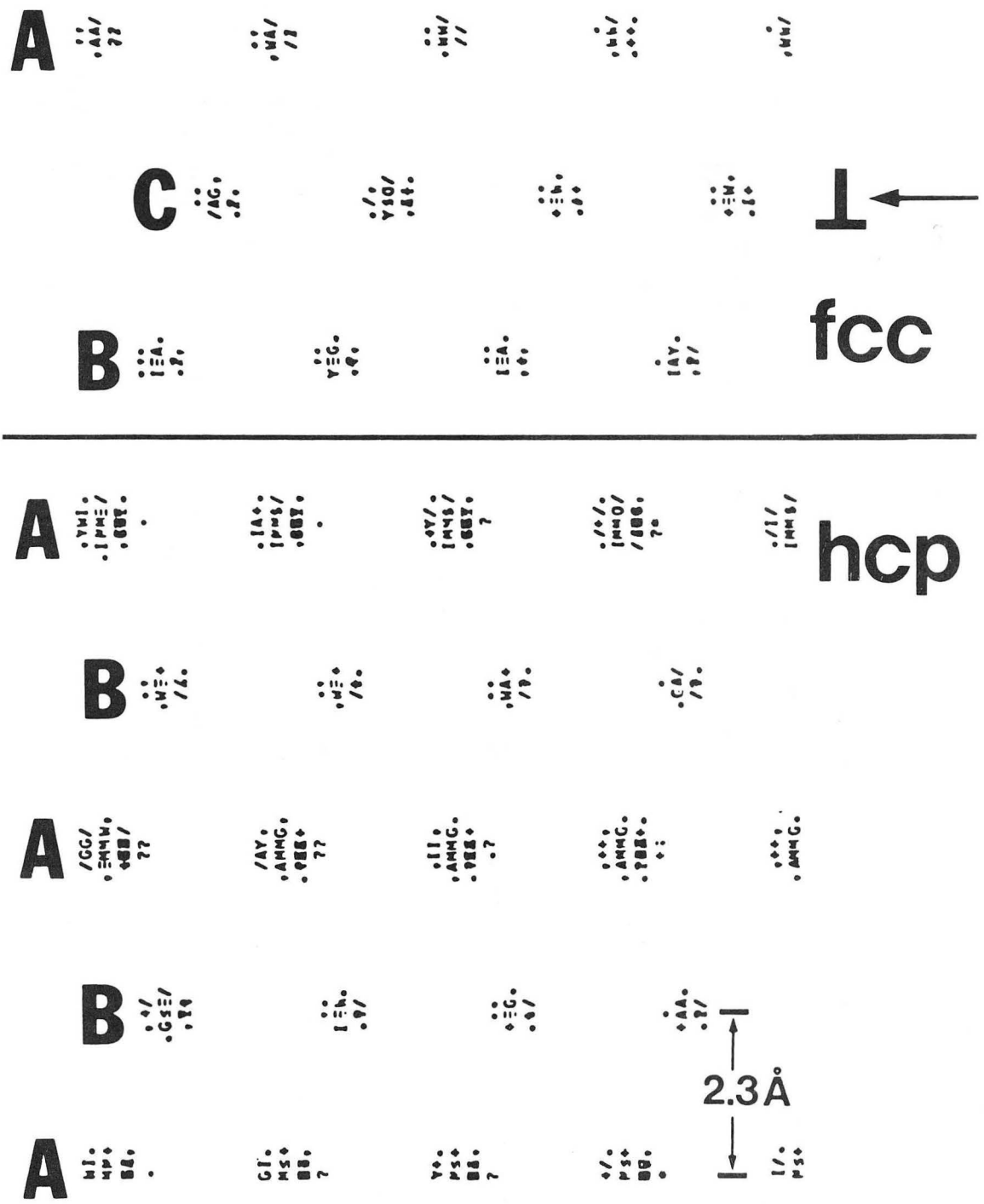

XBL 8511-4500

Fig. 12

LAWRENCE BERKELEY LABORATORY
TECHNICAL INFORMATION DEPARTMENT
UNIVERSITY OF CALIFORNIA
BERKELEY, CALIFORNIA 94720